

EM Implosion Memos

Memo 27

June 2009

Simulation results for 3-layer and 6-layer planar non-uniform launching lens

Prashanth Kumar, Carl E. Baum, Serhat Altunc, Christos G. Christodoulou and Edl Schamiloglu

University of New Mexico

Department of Electrical and Computer Engineering

Albuquerque, NM 87131

Abstract

This paper develops expressions to determine the dielectric constants and width of layers for a planar launching lens. Results of CST simulations for 3-layer and 6-layer cases are presented.

1 Introduction

The planar launching lens is the simplest design. However, analytically, the ray paths are complicated due to reflections at the dielectric boundaries inside the lens. The lens boundary curve and clear time calculations have already been presented in [1]. The next step is to calculate the dielectric constants and widths of various layers. The optimum number of layers can be determined based on results of simulations.

2 Determination of dielectric constants and widths of various layers

The dielectric constants (ϵ_{r_k} for k^{th} layer) and widths of the various layers (d_k for k^{th} layer) are chosen such that every layer has the same *electrical width* i.e. the product $d_k \sqrt{\epsilon_{r_k}}$ is the same for each layer.

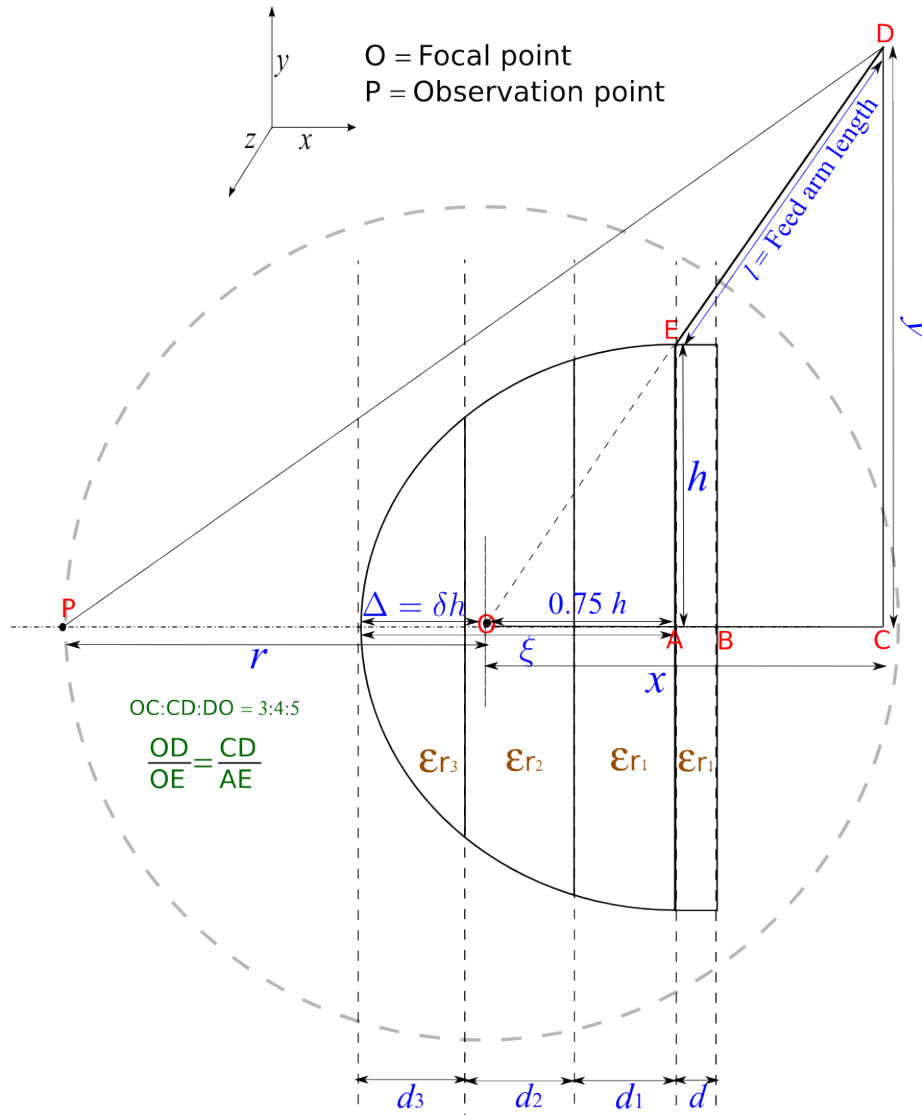


Figure 2.1: Calculations of various dimensions for launching lens

Consider the conventions used in Fig. 2.1 and the generic case of an n -layered lens. Let the ϵ s follow a log-periodic progression such that for n layers, the dielectric constant of the k^{th} layer is $\epsilon_{r_k} = s^{(n-k+1)/n}$ i.e. $\epsilon_{r_1} = s$.

We also want the electrical distances to be constant i.e. for all layers $d_k \sqrt{\epsilon_{r_k}} = C$ where C is a constant. We also have the additional constraint

$$\sum_{k=1}^n d_k = (0.75 + \delta)h \quad (2.1)$$

where h is the radius of the lens where the electrical center of the feed arm intersects the lens.

The equal time condition is:

$$h\sqrt{\epsilon_{r_1}} + r - \frac{5h}{4} = d_1\sqrt{\epsilon_{r_1}} + d_2\sqrt{\epsilon_{r_2}} + d_3\sqrt{\epsilon_{r_3}} + \dots + d_n\sqrt{\epsilon_{r_n}} + r - \Delta = \sum_{k=1}^n d_k\sqrt{\epsilon_{r_k}} + r - \Delta \quad (2.2)$$

This can be simplified using our assumptions (and $\delta h = \Delta$) as

$$h\sqrt{s} - \frac{5h}{4} = \sum_{k=1}^n C - \Delta \Rightarrow s = \left[\frac{Cn}{h} + \left(\frac{5}{4} - \delta \right) \right]^2 \text{ or } C = \frac{[\sqrt{s} - (5/4 - \delta)]h}{n} \quad (2.3)$$

Therefore,

$$d_k = C/\sqrt{\epsilon_{r_k}} = \frac{[\sqrt{s} - (5/4 - \delta)]h}{n\sqrt{\epsilon_{r_k}}} \quad (2.4)$$

Using the constraint on the sum of d 's we can obtain a constraint on the sum of ϵ 's

$$\sum_{k=1}^n \frac{[\sqrt{s} - (5/4 - \delta)]h}{n\sqrt{\epsilon_{r_k}}} = h \Rightarrow \sum_{k=1}^n \frac{\sqrt{s} - (5/4 - \delta)}{n\sqrt{\epsilon_{r_k}}} = (0.75 + \delta) \Rightarrow \sum_{k=1}^n \frac{1}{\sqrt{\epsilon_{r_k}}} = \frac{n(0.75 + \delta)}{\sqrt{s} - (5/4 - \delta)} \quad (2.5)$$

or in terms of s :

$$\sum_{k=1}^n s^{(k-n-1)/2n} = \frac{n(0.75 + \delta)}{\sqrt{s} - (5/4 - \delta)} \quad (2.6)$$

As an example, for a three layered lens where the height=width= h cm i.e. $\delta = \frac{1}{4}$ and $n = 3$ the above equations yield

$$\epsilon_{r_1}, \epsilon_{r_2}, \epsilon_{r_3} = s, s^{2/3}, s^{1/3} = 8.903, 4.296, 2.073 \quad (2.7)$$

$$C = 0.661269h \quad (2.8)$$

$$d_1, d_2, d_3 = C/\sqrt{s}, C/\sqrt{s^{2/3}}, C/\sqrt{s^{1/3}} = 0.222h, 0.319h, 0.459h \quad (2.9)$$

Slope for $\epsilon_{r_1} = s = -0.77$

3 Simulation setup and important CST parameters

This section explains geometries and simulation parameters used in CST. Although the setup is explained with respect to the 3-layer planar case, most parameters are the same in all simulations. Therefore these specifications must be considered as the default unless mentioned otherwise.

3.1 Lens, switch and plug geometries

Figure 3.1 shows the 3-dimensional view of the lens setup with truncated feed arms. The feed arms were truncated to reduce the computational time. However, the length of the feed arms were sufficiently long so that the rays from the tip of the feed arm did not interfere with direct rays from the source in the time of interest (see section 7 in [?] for calculations of important times).

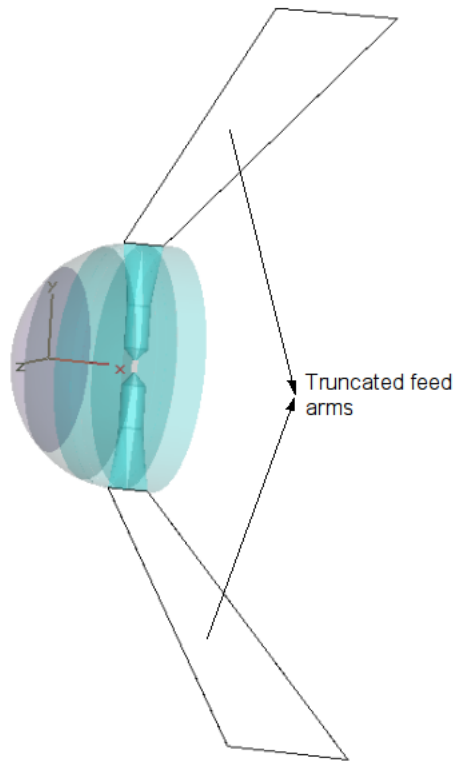


Figure 3.1: 3-dimensional view of simulation setup

Geometrical details of the setup are shown in Fig. 3.2. The height and width of the lens, h , were fixed at 10 cm. The focal point is at the origin of the coordinate system. Distance between the source/switch and the focal point is 7.5 cm. The layer closest to the switch is considered as the first layer. Figure 3.2 also shows a “plug” behind the first layer of the lens. This plug is basically a dielectric cylinder of the same dielectric constant as the first layer of the lens and hence prevents discontinuity for waves originating at the source. The plug was chosen to be 7.5 cm i.e. of sufficient length that the round trip time of a wave travelling through the plug does not interfere with the direct waves from the source in the time of interest (see section 7 in [?] for calculations of important times).

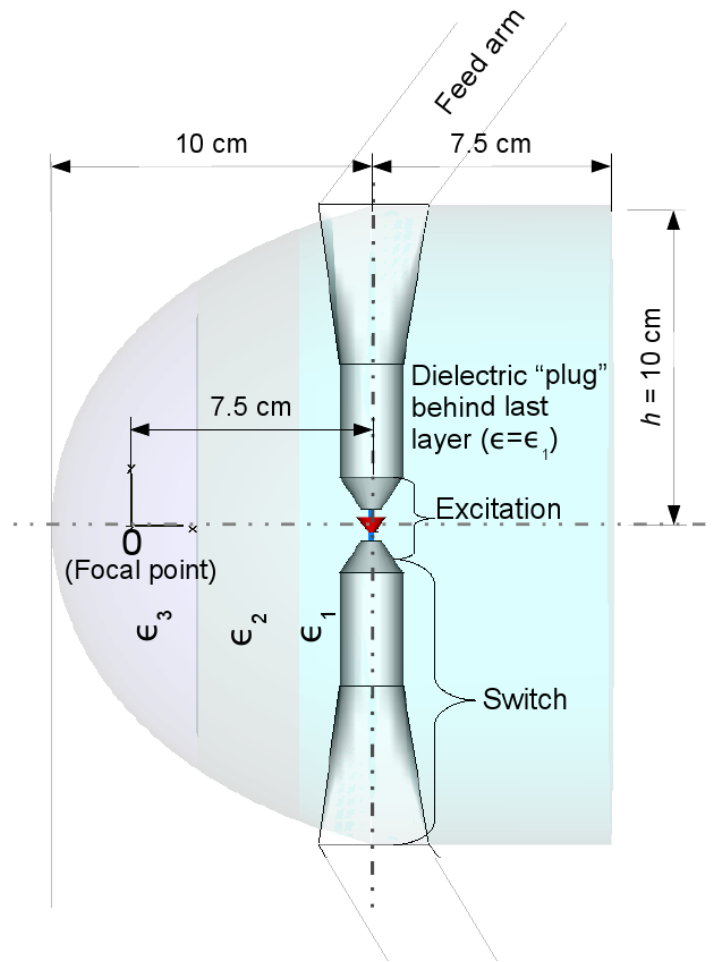


Figure 3.2: Dimensions of lens, switch and plug used in simulations

Dimensions of the switch are shown in Fig. 3.3. The switch is sandwiched exactly in between the first layer of the lens and the plug. The switch gap is 1 cm and the excitation voltage is 1 V.

3.2 Important CST MWS parameters

Important CST MWS parameters used in our simulations:

- Rise time : 100 ps, which corresponds to a wavelength of $(3 \times 10^{10} \text{ cm/s}) \times 100 \text{ ps} = 3 \text{ cm} = 30 \text{ mm}$.
- Lines per wavelength (LPW) = 20
- Frequency range = 0 GHz – 10 GHz
- Switch excitation voltage = 1 V
- Time domain simulation

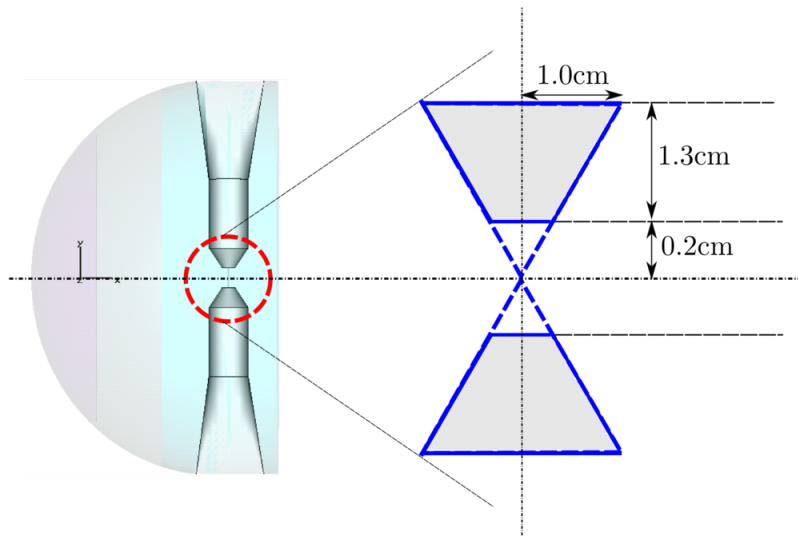


Figure 3.3: Dimensions of switch used in simulations

3.3 Electric field probe orientations

Orientation of various electric-field probes (oriented in the y direction) in the $x-z$ plane are shown in Fig. 3.4. Probes were placed 15° apart with a probe at 127° (at the feed arm angle). Our initial concern is the time of arrival of waves at all the probes and therefore observations in one plane should suffice as a starting point. Also, since the lens is rotationally symmetric, one should observe similar responses in the other planes.

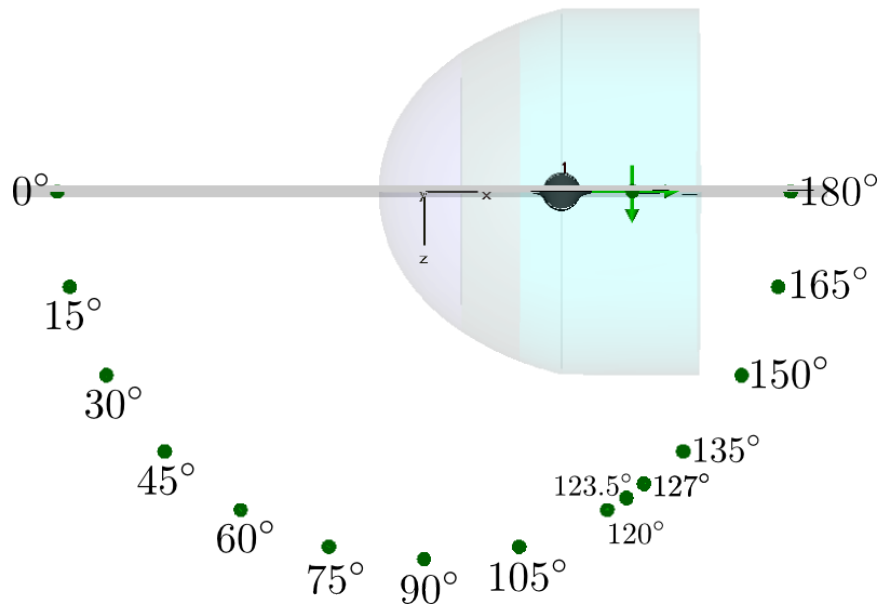


Figure 3.4: Orientation of various electric field probes with respect to lens to measure electric fields in the $x-z$ plane.

4 Simulation results for 3-layer case

The dielectric constants and widths of the layers calculated using equation 2.6 in section 2 are tabulated below ($h = 10$ cm)

| Layer | ϵ_r | d (cm) |
|-------|--------------|----------|
| 1 | 8.903 | 2.22 |
| 2 | 4.296 | 3.19 |
| 3 | 2.073 | 4.59 |

A perspective view of the lens is shown in Fig. 4.1.

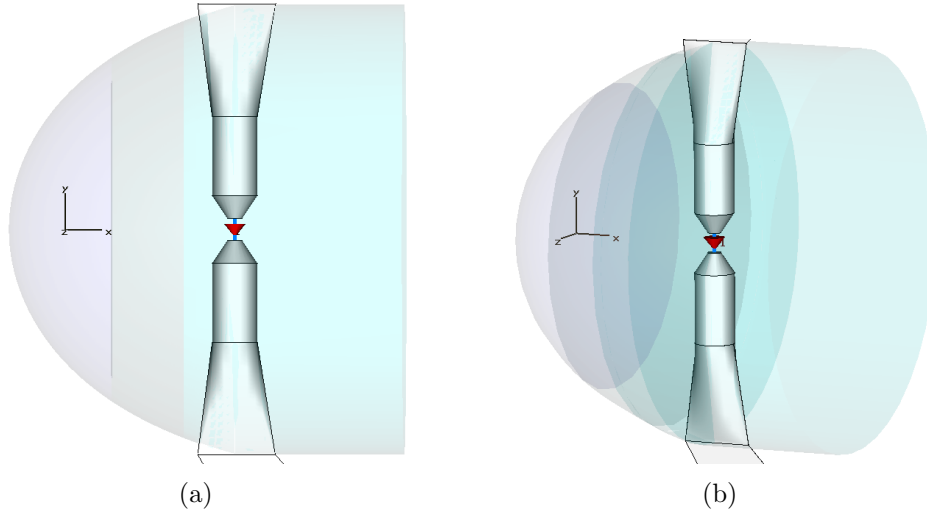


Figure 4.1: Front and perspective views of 3-layer planar lens

Results for the 3-layer planar lens are shown in Fig. 4.2. Note that the lens boundary curve has been fixed at $\theta' = 0^\circ$ and $\theta' = 90^\circ$ (in the r', θ' coordinate system – see [1]). Therefore, theoretically we expect the responses at 0° and 127° to overlap each other. However this is *not* observed in Fig. 4.2. The 127° response *does* “turn back” i.e. arrive later than the 90° response. There is approximately a 130 ps spread between the 0° and 90° responses which is much greater than the tolerable time difference of 10 ps. Increasing the dielectric constants of various layers of the lens could compensate for the early arrival of the 127° ray compared to the 0° ray. However, it is not simple to predict the effect of variation of dielectric constants on the results, since the ray paths are complicated inside the lens. Rays from different paths may interfere with the direct ray in the time domain of interest (100 ps). Simulations were done where the dielectric constants of all layers were multiplied by 1.2 and 4.0. The 127° and 0° responses *did* overlap but the 130 ps spread in time did not change. Besides, use of such high dielectric constants defeats the purpose of using a non-uniform lens.

5 Simulation results for 6-layer case

The dielectric constants and widths of the layers calculated using equation 2.6 in section 2 are tabulated below ($h = 10$ cm)

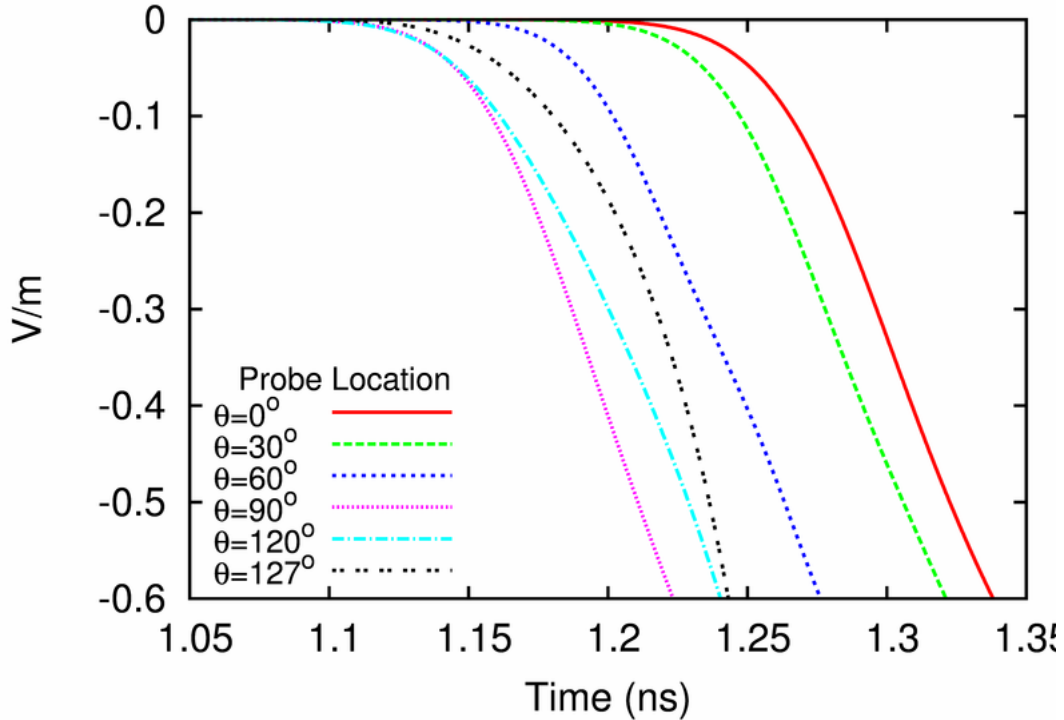


Figure 4.2: Electric field results for 3-layer lens design at various angles in the $x - z$ plane for the probe setup shown in figure 3.4.

| Layer | ϵ_r | d (cm) |
|-------|--------------|----------|
| 1 | 7.414 | 1.06 |
| 2 | 5.310 | 1.25 |
| 3 | 3.802 | 1.47 |
| 4 | 2.723 | 1.74 |
| 5 | 1.950 | 2.06 |
| 6 | 1.396 | 2.43 |

The front and perspective views of the lens are shown in Fig. 5.1. Compared to the 3-layer case, one would expect that increasing the number of layers would improve the results, due to the smoother dielectric variation. However Fig. 5.2 seems to indicate otherwise. Results are similar to the 3-layer case, only that in this case the response turns around at 120° instead of 90° . The time difference between the 120° and 0° responses (extrema) is still of the order of 130 ps. It is possible that rays following “alternate paths” interfere with direct rays causing the earlier arrival times observed at larger angles. However, it is extremely difficult to analytically verify if this is the case (hence the need for simulations!). Simulations with dielectric constants of all layers multiplied by 2.0, 4.0 and 6.0 yield results similar to the corresponding 3-layer cases. The time difference in all these simulations was of the order of 130 ps as in the 3-layer case.

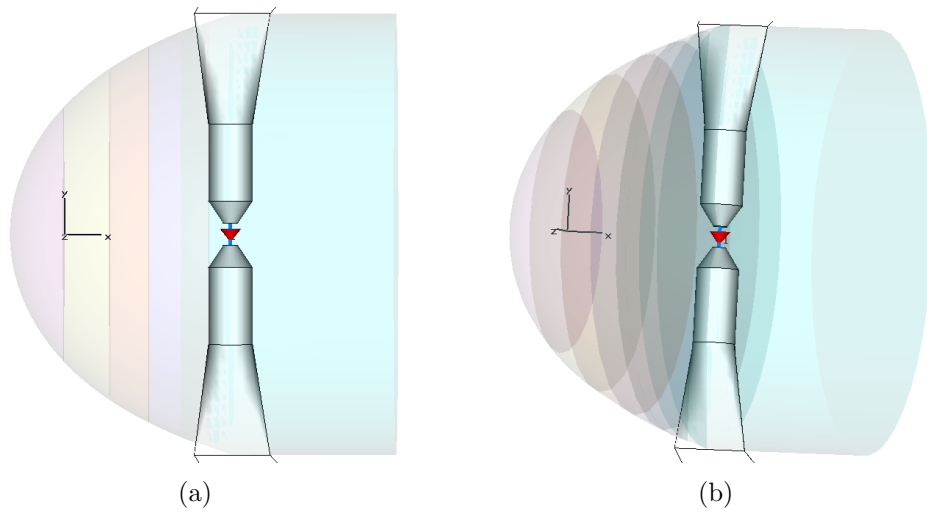


Figure 5.1: Front and perspective views of 6-layer planar lens

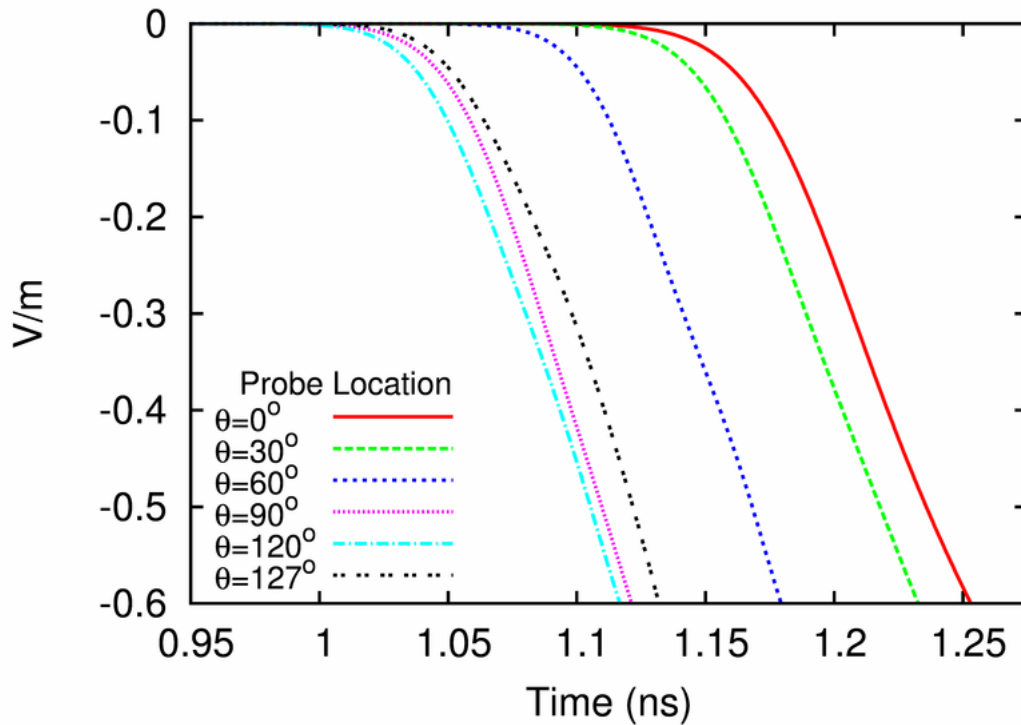


Figure 5.2: Electric field results for 6-layer lens design at various angles in the $x - z$ plane for the probe setup shown in figure 3.4.

6 Conclusions

Analytical calculations for determination of the dielectric constants and widths of the dielectric layers for a planar non-uniform launching lens have been presented. Simulation results for the 3-layer and 6-layer cases have been presented. There does not seem to be much difference in responses when the number of layers are increased. However, a spread of the order of 130 ps is

observed in the responses for both the 3-layer and 6-layer cases. This is much greater than the tolerable time difference of 10 ps. It is difficult to speculate the causes for the responses obtained as the analytical determination of ray paths within the lens is a very complicated problem. We suspect that the most likely cause of the observed discrepancies is due to numerical errors in CST.

References

- [1] Prashanth Kumar, Serhat Altunc, Carl E. Baum, Christos G. Christodoulou, Edl Schamiloglu, “Analytical considerations for curve defining boundary of a non-uniform launching lens.” EM Implosion Memo 26, June 2009.